水工学論文集　第36巻　1992年２月

2-D SEDIMENT TRANSPORT SIMULATION IN NATURAL STREAMS

By Ivan Botev †, Nobuyuki Tamai ‡ and Yoshihisa Kawahara ††

River bed evolution during a flood event is modeled in a quasi-steady approach using a 2-D depth-averaged numerical model. It is concluded that, with respect to the numerical solution, more significant are the accuracy of flow field computations and the precision achieved in approximating the bed geometry rather than differences in sediment transport rate formulas.

Keywords: bed evolution, numerical simulation, natural stream

1. Introduction

Being of a relatively simple concept and easy to use, 2-D numerical models have been widely used to handle a wide range of real-life problems with variable success. The present study classifies some of the major factors contributing to improve simulation accuracy in a natural stream of highly irregular cross-sectional shape and complex plane configuration. In particular, the study investigates bed evolution occurring in a river confluence during the propagation of a flood wave. Several numerical experiments have been carried out by means of a 2-D depth-averaged model. The experiments were aimed to achieve good agreement with observed changes in river bed topography during a real flood event and focused the analysis of sediment transport driving forces. Eventually, the series of conclusions reached in the study have led to the formulation of explicit recommendations for the use of 2-D models in engineering analysis of flood events on movable bed. Within the present study, the implementation of these recommendations has significantly improved the accuracy of the numerical results and hence, the reliability of bed evolution simulation.

2. Structure of the Model

The model is designed as a three-component system (Fig.1). Each component is given a name related to its function. For instance GRID supplies the system with a boundary-fitted curvilinear computational grid laid on the current water surface. FLOMOD denotes a solver for the pressure and depth averaged velocity field, whereas SEDMOD simulates channel bed evolution under the flow patterns generated by FLOMOD.

In order to simulate flood wave propagation in a quasi-steady approach, that is, as a sequence of steady flow computations, the flood wave stage and discharge hydrographs have been approximated using a step function. At each step of the hydrographs the system performs in a sequential mode grid generation, flow and sediment transport modeling.

†Obayashi Corporation, Technical Research Institute, Researcher,(Kiyose-shi, Tokyo 204)
‡Dept. of Civil Engineering, Univ. of Tokyo, Professor,(Hongo, Bunkyo-ku, Tokyo 113)
††Dept. of Civil Engineering, Univ. of Tokyo, Associate Professor

To prolong sediment transport modeling intervals and to partially compensate for decoupling of flow and sediment transport modeling, SEDMOD relies on STUDH's velocity adjusting technique by McAnally[1]. The technique allows velocities to be "recalculated" or adjusted at each time step within the sediment transport model and to account in this way for the latest depth changes. To do this, the bed elevation at the center of each computational control volume is reformed at each time step by the computed amount of deposition or erosion. The adjustment of velocities performed by SEDMOD consists in increasing/decreasing the velocity at each volume center, each time step, as deposition/erosion occurs. The new velocity component U corresponding to the newly computed flow depth H is adjusted using the relation $U = U_a H_a / H$, where U_a and H_a are the initial velocity component and depth at the current time step.

3. Flow Modeling

The steady shallow water equations expressed in orthogonal curvilinear coordinates were used for flow simulation. The equations are valid under the assumption that vertical shear stresses and accelerations of water are negligibly small compared with the gravitational acceleration. With respect to the commonly used shallow water equations expressed in rectangular coordinates, the momentum equations for the present numerical model are expanded with extra terms accounting for the curvature of the transformation and the centrifugal acceleration of the motion. The set of equations is expressed as [2),3)]:

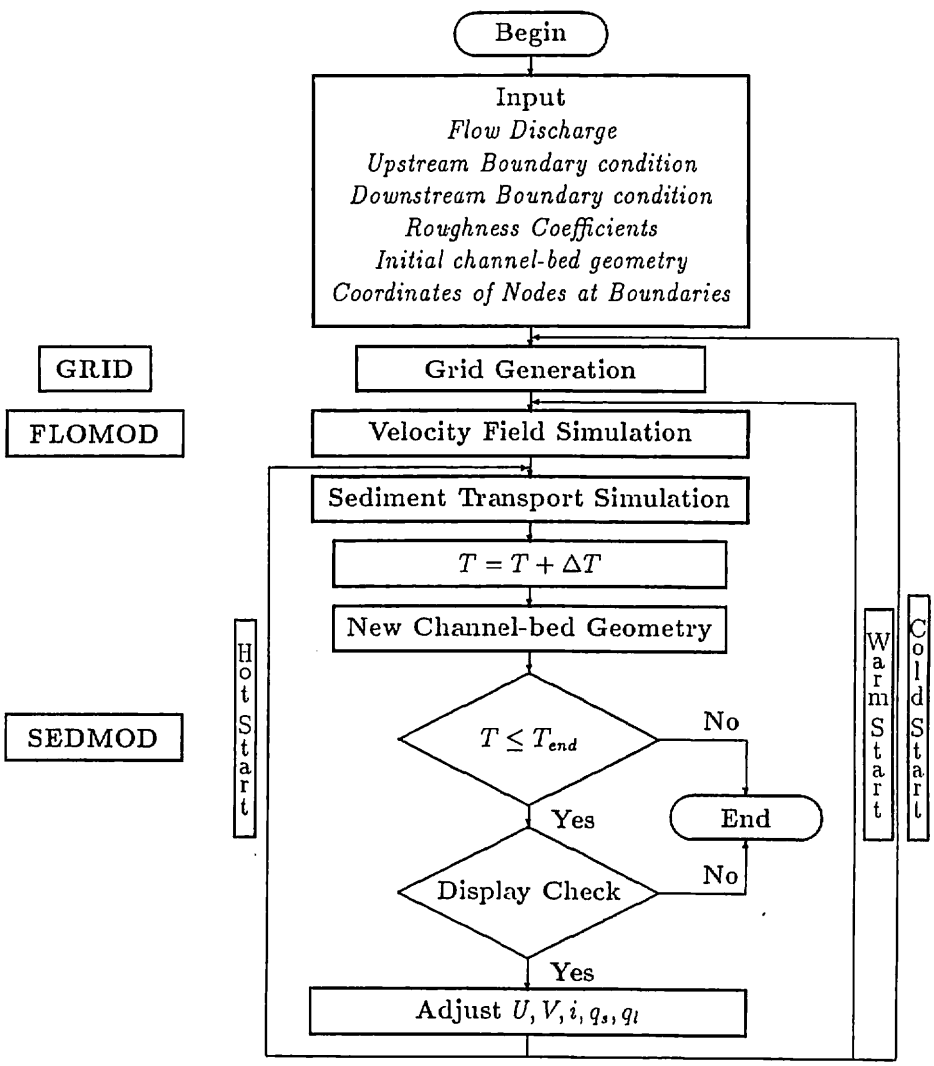

Figure 1: General flowchart

Continuity equation

$$\frac{1}{h_1 h_2}\frac{\partial}{\partial \xi}\{HUh_2\} + \frac{1}{h_1 h_2}\frac{\partial}{\partial \eta}\{HVh_1\} = 0 \tag{1}$$

Conservation of momentum in the ξ direction

$$\frac{U}{h_1}\frac{\partial U}{\partial \xi} + \frac{V}{h_2}\frac{\partial U}{\partial \eta} + \frac{UV}{R_\xi} - \frac{V^2}{R_\eta} + CU + \frac{g}{h_1}\frac{\partial z}{\partial \xi} = \frac{\epsilon}{h_1}\frac{\partial}{\partial \xi}A - \frac{\epsilon}{h_2}\frac{\partial}{\partial \eta}F \tag{2}$$

Conservation of momentum in the η direction

$$\frac{U}{h_1}\frac{\partial V}{\partial \xi} + \frac{V}{h_2}\frac{\partial V}{\partial \eta} + \frac{UV}{R_\eta} - \frac{U^2}{R_\xi} + CV + \frac{g}{h_2}\frac{\partial z}{\partial \eta} = \frac{\epsilon}{h_2}\frac{\partial}{\partial \eta}A + \frac{\epsilon}{h_1}\frac{\partial}{\partial \xi}F \tag{3}$$

where

$$C = \frac{g n^2}{H^{4/3}}\sqrt{U^2+V^2}, \qquad \frac{1}{R_\xi} = \frac{1}{h_1 h_2}\frac{\partial h_1}{\partial \eta}, \qquad \frac{1}{R_\eta} = \frac{1}{h_1 h_2}\frac{\partial h_2}{\partial \xi} \tag{4}$$

$$A = \frac{1}{h_1 h_2}\{\frac{\partial}{\partial \xi}(Uh_2) + \frac{\partial}{\partial \eta}(Vh_1)\}, \qquad F = \frac{1}{h_1 h_2}\{\frac{\partial}{\partial \xi}(Vh_2) - \frac{\partial}{\partial \eta}(Uh_1)\} \tag{5}$$

with h_1, h_2 - transformation coefficients corresponding with the local grid size respectively in ξ and η directions, H - depth of flow, g - acceleration of gravity, n - Manning's roughness coefficient, U and V - depth-averaged velocity components respectively in ξ and η directions, ξ, η - horizontal coordinates in the transformed domain and ϵ - effective kinematic viscosity.

The depth-averaged flow computations were carried out by the SIMPLE algorithm [4]. The simulation was conducted on a space staggered grid by means of an upwind finite-difference scheme. The resulting set of equations was solved under appropriate boundary conditions [5] by means of the TDMA algorithm and yielded a solution in terms of the primitive variables U, V and p. Pressure p that does not appear explicitly in the above set of equations was treated via a modified pressure correction equation (called depth correction equation) as explicated in detail by Weerakoon [6].

4. Sediment Transport Modeling

Bed evolution resulting from sediment transport was simulated by integrating numerically the equation of continuity for total load in the form:

$$q_{s_\xi}\frac{y_\eta}{J} - q_{s_\eta}\frac{y_\xi}{J} - q_{l_\xi}\frac{x_\eta}{J} + q_{l_\eta}\frac{x_\xi}{J} = -(1-\lambda)\frac{\partial z_b}{\partial t} \tag{6}$$

where subscripts ξ and η stand for the partial derivatives with respect to ξ and η, J being the determinant of the inverse Jacobian matrix of the transformation, z_b - the bottom surface elevation, t - time and λ - the sediment porosity. Variables q_s and q_l denote total load per unit-width per unit time in the longitudinal (streamwise) and lateral direction, respectively. The reference of q_s and q_l as total load emphasizes that the terms include contributions from bed-load and suspended load.

Equation (6) is directly discretized in the transformed computational space (ξ, η) using an explicit central finite-difference approximation. The location of the discretized variables in the transformed plane is in accordance with the current practice for staggered-grid formulations (Patankar and Spalding[7], Patankar[4], Van Doormal and Raithby[8]).

The formula of Meyer-Peter and Müller and Bagnold's formula were used to determine the bed-load sediment transport rate in the longitudinal direction. However, no restrictions are imposed for the use of any other formulas.

The velocity components near the river bed were defined as $u' = \gamma U$ and $v' = \gamma V$ with $\gamma = 3(1-\beta)/(3-\beta)$ and $\beta = 3/(C+1)$, C denoting a non-dimensional Chezy number. The secondary flow occurring in river bends was accounted for by means of an additional velocity component in the lateral direction expressed as $v'' = 7.0Hu'f_0/r$, where f_0 is a function of η and describes the distribution of the spiral flow near the bed [9] and r are the local radii of curvature defined within each computational

control volume. The sediment transport rate in the lateral direction (per unit river length) was evaluated according to Shimizu and Itakura [10] as:

$$q_l = q_s \left(\tan \delta - \sqrt{\frac{\tau_{*_c}}{\mu_s \mu_k \tau_*}} \frac{\partial z_b}{\partial \eta} \right) \tag{7}$$

In the above expression $\tan \delta = (v' + v'')/u'$, where δ is the angle at which the flow near the bottom deviates under the effect of v'' from the streamwise direction. Other notations used are $\tau_* = u_*^2/(sgD)$ - non-dimensional bed shear stress, $\tau_{*_c} = u_{*_c}^2/(sgD)$ - Iwagaki's non-dimensional critical shear stress [11], u_* - shear velocity, $s = (\rho_s - \rho)/\rho$, D - mean diameter of sediment particles, ρ - density of water, ρ_s - mass density of sediment, μ_s - static friction factor and μ_k - kinematic friction factor.

With respect to sediment transport conceptualization, the present model differentiates actual sediment transport capacity from the equilibrium one and simulates spatial delay effects in sediment loading. The latter concept is realized by adopting a bed-load loading law in the form $q_a = \tanh[a_1(1 + a_2)]\, q_s$ where q_a is the actual sediment transport rate, q_s - the equilibrium sediment transport rate and a_1, a_2 - calibration constants. The above bed-load loading law is in conformity with the current practice as reported by Holly[12]. It models a spatial delay in sediment loading, whereby the actual bed-load transport asymptotically approaches the theoretical equilibrium value.

5. Discussion of the Results

The flow model calibration, conducted by Weerakoon[6] under observed upstream discharge distribution and downstream depths, yielded a set of $n = 0.040$ and $n = 0.060$ as representative for the roughness coefficient respectively in the main channel and the flood plain. The effective viscosity ϵ was assigned a value of $1\text{m}^2/\text{s}$. For the sediment transport model the mean particle diameter D_m was assigned a value of 1mm, the specific weight of immersed sediment particles γ_s being $1.5 \times 10^4\ \text{N/m}^3$ and the sediment porosity $\lambda = 0.4$. Suspended sediment was not included in the continuity equation for sediment transport upon consideration that for bed level change its contribution is not significant.

It was observed that pressure oscillations appear exclusively inside thalweg bends with strong curvature and abrupt changes in cross-sectional shape when the shear velocity was formulated by the energy gradient. In river reaches where the conditions mentioned above are present, damping pressure oscillations using an uniform energy gradient that represents the reach mean value gives good agreement with observations for cross sections located at the entrance and exit of thalweg bends but fails to reproduce bed evolution within the thalweg.

Introducing the commonly accepted assumption that near-the-bed lateral velocities - v'', representing the effect of secondary flow in a bend, are always directed toward the inner bank of the stream gives only a partial solution for recreating observed changes inside thalweg bends. The introduced assumption suggests that in a bend lateral transport is dominantly toward the inner bank. However, this may not always be true in natural streams where flow and channel curvature often differ or lag behind each other. Moreover, deviation angles δ computed using the formula given in Section 4 do not always direct near-the-bed velocities toward the inner bank. Finally it is worth noting that in comparison with the well-known Rozovskii formula, the modeling system has predicted for near-the-bottom velocities larger angles of deviation δ from the tangential direction.

In consequent runs therefore, the shear velocity formulation based on energy gradient - $u_* = \sqrt{gHI}$ was replaced with the expression $u_* = n\sqrt{g(U^2 + V^2)}/H^{1/6}$. Accordingly, sediment transport capacities were protected against pressure and energy gradient oscillations but the lateral sediment transport rate inside thalweg bends remained poorly approximated when compared with observations. In view of a better agreement with observations the computational grid was regenerated with dense concentration of grid lines in regions of transition between thalweg and flood plain. In addition, the local radii of curvature were redefined on real geometry basis rather than on streamlines (curvilinear coordinates) curvature. Indeed, from the very beginning of the simulation process streamlines have been controlled to follow the thalweg but this requirement was not fully met because of the necessity to concurrently preserve grid orthogonality.

As a direct consequence of radii of curvature refinement and grid relocation lateral sediment transport was activated to such an extent where a satisfactory agreement with observations could be reached. The results of a numerical simulation performed on a grid fitted to the thalweg of the stream (high density

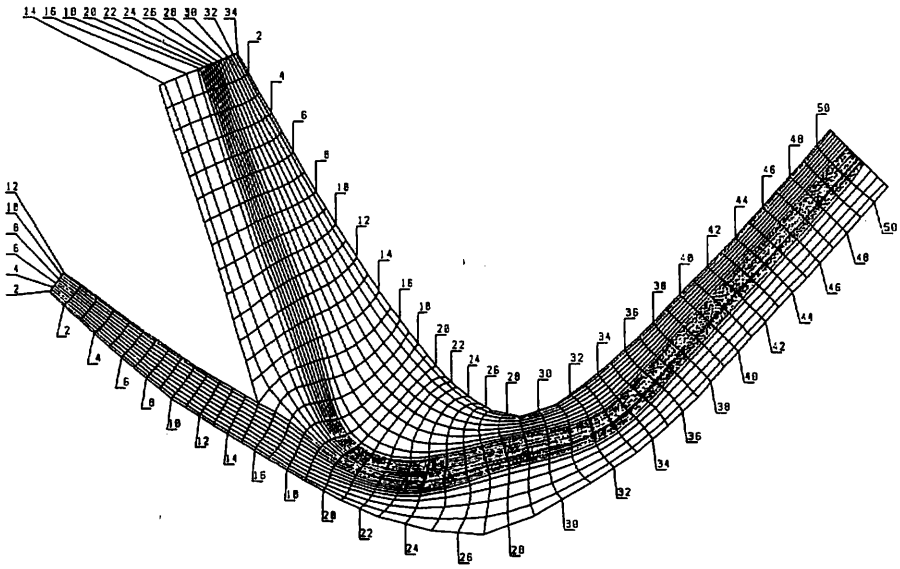

Figure 2: Computational grid generated to fit the thalweg of the stream.

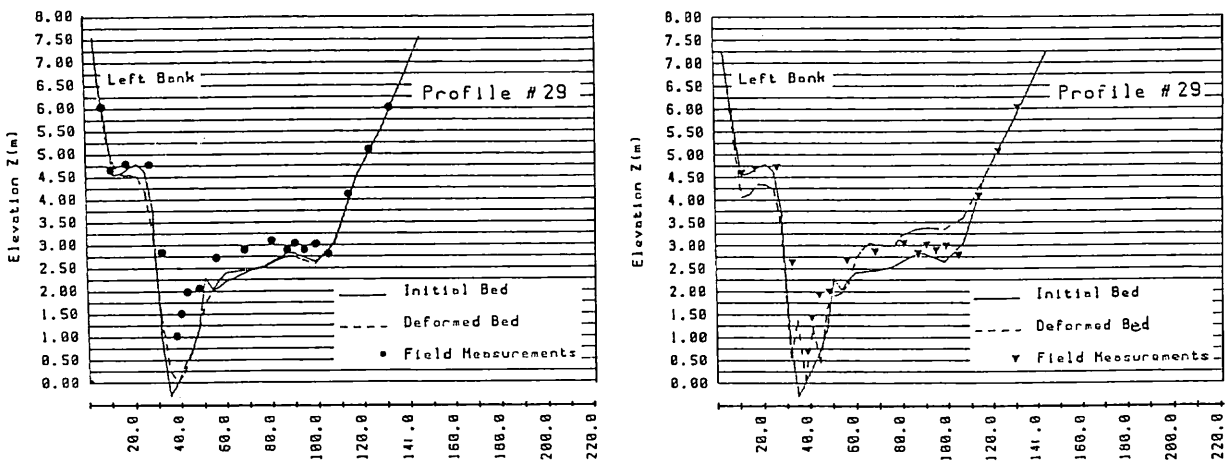

(a) No refinement (b) Refinement

Figure 3: The influence of local radii of curvature refinement

mesh on Fig.2) in conjunction with radii refinement are illustrated on Fig.3(b). The influence of changes brought to local radii of curvature is easily evaluated by comparing the results shown on Fig.3(a) and 3(b) corresponding to transverse section #29 on Fig.2.

Further calibration runs focused on modeling mixing layer and river bed armoring, the alternate use of different sediment transport rate formulas and the introduction of spatial delay effects in sediment loading. The thickness of the mixing layer was taken proportional to flow depth for any specific location and, meanwhile, was allowed to decrease progressively in time as the discharge becomes smaller. Under these constraints the thickness of the mixing layer was varied in the range $0.15 \sim 0.05$ m. It was found that assuming armoring at lower discharges has small effect on bed evolution, as bed transformation decreases in intensity. Moreover, introducing the bed-load loading law given in Section 4 yielded results demonstrating that the presence of mixing layer and armoring effect may be simulated by means of bed-load loading control. The advantage that results consists in eliminating uncertainties in defining mixed layer thickness and its local distribution. For the bed-loading law used in the calibration of the model the calibration constant a_1 was taken equal to 0.5, while a_2 was varied from zero to unity from the upstream boundary toward the downstream direction.

Finally, the comparison of results obtained under identical simulation conditions by means of Bagnold's

formula and the formula of Meyer-Peter and Müller demonstrated differences in river bed evolution of significantly reduced magnitude when compared to these originated by the refinement of radii of curvature or changes in the computational grid distribution.

6. Conclusions

The simulation of bed evolution following a major flood event has been conducted in a quasi-steady approach with the flood hydrographs being approximated by a step function. Local radii of curvature, pressure oscillations, grid distribution and sediment transport rate formulas have been subject to sensitivity analysis.

For instance, numerical solutions have been found sensitive to radii of curvature, pressure oscillations, computational grid distribution, mixing layer thickness and sediment transport rate formulas listed in order of influence. The conclusion emphasizes that, with respect to the numerical solution more significant are the accuracy of flow field computations and the precision achieved in approximating the bed geometry rather than differences in sediment transport rate formulas. Thus, grid generation has a significant impact on sediment transport simulation and may shift the attention of river engineers from the "tuning" of transport rate formulas towards the issue of representing with greater accuracy river bed geometry.

In conclusion, depth-averaged models should be applied to compound channels with great caution. Abrupt longitudinal and transverse changes in geometry (for instance the interface between the thalweg and the flood plain) are a violation of the initial assumptions and may weaken the convergence of the numerical solution. However, a non-uniform, locally refined, boundary-fitted curvilinear coordinate system combined with the benefits of staggered grid formulation for both flow and sediment transport simulation allow to treat the problem by preserving the stability of the numerical procedure. Numerical solutions obtained under these conditions stay within the precision required for most engineering applications.

References

1. McAnally, W. H.: STUDH:A Two-Dimensional Numerical Model for Sediment Transport. *Proc. of the Int. Symp. on Sediment Transport Modeling, New Orleans, Louisiana,* 659-664,1989.
2. Wijbenga,J.H.A.: Determinations of flow patterns in rivers with curv ilinear coordinates, Proc. 21st IAHR Congress, Melbourne, 2, 132 -138,1985.
3. Willemse,J.B.T.M., Stelling,G.S. and Verboom,G.K.: Solving the shal low water equations with an orthogonal coordinate transformation, Delft Hydraulics Laboratory Report No 356,1986.
4. Patankar,S.: Numerical Heat Transfer and Fluid Flow, Hemisphere Publishing Corporation, McGraw Hill Book Co., New York, N.Y., 195p.,1980.
5. Vreugdenhil,C.B. and Wijbenga,J.H.A.: Computation of flow patterns in rivers, Journal of the Hydraulics Div., ASCE, 108(11), 1296-1310,1982.
6. Weerakoon,S.B.: Flow structure and bed topography in river confluences, Thesis submitted to the University of Tokyo in partial fulfillment of the requirements for the Ph.D degree, 1990.
7. Patankar, S., and Spalding, D.: A calculation procedure for heat, mass and momentum transfer in three-dimensional parabolic flows, *Int. J. Heat and Mass Transfer,* 15, 1787-1806,1972.
8. Van Doormaal, J. P. and Raithby, G. D.: Enhancements of the SIMPLE Method for Predicting Incompressible Fluid Flows, *Numerical Heat Transfer,* 7, 147-163,1984.
9. Kikkawa,H., Ikeda,S. and Kitagawa,A.: Flow and Bed Topography in Curved Open Channels, Journal of the Hydraulics Div., ASCE, 102(9), 1327-1342,1976.
10. Shimizu,Y. and Itakura,T.: Calculation of bed variation in alluvial channels, Journal of the Hydraulics Engrg., ASCE, 115(3), 367-384,1989.
11. Iwagaki,Y., in Suirikoushikishu, Japan Society of Civil Engineers(ed.),1971.
12. Holly, F. M. Jr.: Numerical simulation in alluvial hydraulics, *5th Congress of the Asian and Pacific Regional Division of the IAHR, Seoul, Korea.* 79-99,1986.